Indonesian Journal of Electrical Engineering and Computer Science
Vol. 2, No. 2, May 2016, pp. 351 ~ 358
DOI: 10.11591/ijeecs.v2.i2.pp351-358

Experimental Multipath Delay Profile of Underwater Acoustic Communication Channel in Shallow Water

Yasin Yousif Al-Aboosi[1,2] Ahmad Zuri Sha'ameri[1]
[1]Faculty of Electrical Engineering, Universiti Teknologi Malaysia, 81310, Skudai, Johor, Malaysia
[2]Faculty of Engineering, University of Mustansiriyah, Baghdad, Iraq
*Corresponding author, e-mail: ymyasin2@live.utm.my

Abstract

The shallow water channel is an environment that is of particular interest to many research fields. An underwater acoustic channel is characterized as a multipath channel. Time-varying multipath propagation is one of the major factors that limit the acoustic communication performance in shallow water. This study conducts two underwater acoustic experiments in Tanjung Balau, Johor, Malaysia. A transducer and a hydrophone are submerged at different depths and separated by different distances. Linear frequency modulated (LFM) pulses are chosen as the main transmit signal for the experiments. The cross-correlation between the transmitted and received signals represents the impulse response of the channel (multipath profile). The results show that the amplitude of the successive paths will not rapidly decline, and vice versa, when the distance between the sender and the receiver increases. Moreover, the time difference between the different paths will be small in the case of distance increase. In other words, the successive paths will converge in time.

Keywords*: Underwater communications, multi-path, shallow water channel, Ray model, correlation*

1. Introduction

Increasing interest in the defense sector, off-shore oil industry, and other commercial operations in the underwater environment makes underwater research more popular. Electromagnetic waves in the underwater environment are exposed to high attenuation and can only travel very short distances. Therefore, the only way that navigation, communication, and other wireless applications can be done is through acoustic methods [1-3]. The underwater acoustic communication channel (UW-ACC) is difficult to employ and has inherent problems. The difficulty comes from channel characteristics, such as attenuation, multipath fading, time-varying characteristics, and channel inhomogeneities [4]. The attenuation of sound in the ocean is a frequency-dependent process. Hence, the ocean acts as a low-pass filter [5]. The underwater channel shows inhomogeneities in speed, temperature, and salinity [1]. These variables may also change in time and may be different for the same depth of different places. Therefore, the channel impulse response changes both spatially and temporarily [4, 6].

Multipath occurs in UW-ACC because of reflections and refractions. Reflections occur at the bottom and the underwater channel surface, whereas refractions occur because of sound channels created by the sound speed inhomogeneities. The number of multipaths reaching the receiver side can be very large. However, the multipath under noise level is ignored [2, 7]. Multipath signals generally represent acoustic energy loss. However, the inter-symbol interference (ISI) will also be detrimental at the receiver in communication systems because it can significantly increase the error rate of the received signal. The time difference between the last arrival path over the noise level and the synchronized path in the channel that suffers from the multipath is called delay spread [1]. The length of this delay spread in digital communication systems without equalization places a lower bound on the duration of a symbol T_s or an upper bound on the data rate of the system that must be used to avoid channel-induced ISI [4, 8]. This study aims to determine the multipath profile of the UW-ACC in shallow water at a different range.

Received February 29, 2016; Revised April 25, 2016; Accepted May 1, 2016

2. Underwater Channel Characteristics

This section focuses on some parameters of the UW-ACC that affect the acoustic signal propagation from the transducer to the hydrophone.

2.1. Signal Attenuation

An acoustic signal underwater experiences attenuation due to spreading and absorption. Path loss is the measure of the lost signal intensity from the projector to the hydrophone. Spreading loss is due to the expanding area that the sound signal encompasses as it geometrically spreads outward from the source [9].

$$PL_{spreading}(R) = k * 10\log(R)\ dB \quad (1)$$

where *R* is the range in meters and *k* is the spreading factor. When the medium in which signal transmission occurs is unbounded, the spreading is spherical and the spreading factor $k = 2$; whereas in bounded spreading, it is considered as cylindrical $k = 1$. In practice, a spreading factor of $k = 1.5$ is often considered [2].

The absorption loss is a representation of the energy loss in form of heat due to viscous friction and ionic relaxation that occur as the wave generated by an acoustic signal propagates outwards; this loss varies linearly with range as follows [9]:

$$PL_{absorption}(R, f) = 10\log\big(\alpha(f)\big) * R\ dB \quad (2)$$

where r is range in kilometres and $\alpha\ (f)$ is the absorption coefficient. The absorption coefficient for frequencies above a few hundred Hz can be expressed empirically using Thorp's formula [10], which defines $\alpha\ [dB/m]$ as a function of $f\ [kHz]$.

$$\alpha(f) = \left(0.11\frac{f^2}{f^2+1} + 44\frac{f^2}{f^2+4100} + 2.75.10^{-4}f^2 + 0.0003\right).10^{-3} \quad (3)$$

Total path loss is the combined contribution of both the spreading and absorption losses [1].

$$Total\ Path\ Loss = k * 10\log(R) + 10\log\big(\alpha(f)\big) * R \quad (dB) \quad (4)$$

Since the path losses, expressed in dB, must be returned to its natural value.

$$L_A(R) = 10^{-\left[{total\ path\ loss}/{10}\right]} \quad (5)$$

As seen in Figure 1, the path loss is proportional to the operating frequency. Figure 2 shows the path loss versus the range at different frequencies, the path loss increases with distance and frequency.The shallow water underwater acoustic channel has higher values of attenuation than the deep water underwater acoustic channel [2]; while transmission loss increases with distance and frequency for both.

2.2. Sound Speed

The speed of sound in seawater is a fundamental oceanographic variable that determines the behavior of sound propagation in the ocean. Many empirical formulas have been developed over the years for calculating sound speed using values of water temperature, salinity, and pressure/depth. A simplified expression for the sound speed was given by Medwin [3]:

$$c = 1449.2 + 4.6T - 0.055T^2 + 0.00029T^3 + (1.34 - 0.01T)(S - 35) + 0.016d \quad (6)$$

where *c* is the speed of sound in seawater, *T* is the water temperature (in degrees Celsius), *S* is the salinity (in parts per thousand) and *d* is the depth (in meters).

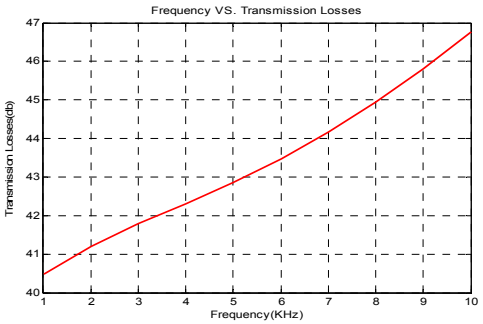

Figure 1. Transmission loss as a function of frequency

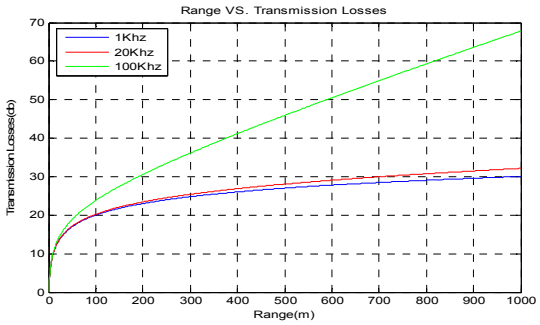

Figure 2. Transmission loss as a function of range

3. Ray Model

The geometry of multipath propagation is important for communication systems which use array processing to suppress multipath. The design of such systems is accompanied by the use of a propagation model for predicting the multipath configuration. Acoustic propagation in the ocean is governed by the wave equation. As solutions to the wave equation are difficult to find in general cases, approximations are often used to model propagation [11, 12]. The ray theory provides one such approximation. The shallow water channel was modeled as a Pekeris waveguide, consisting of an isovelocity layer over an isovelocity half-space as shown in Figure 3.

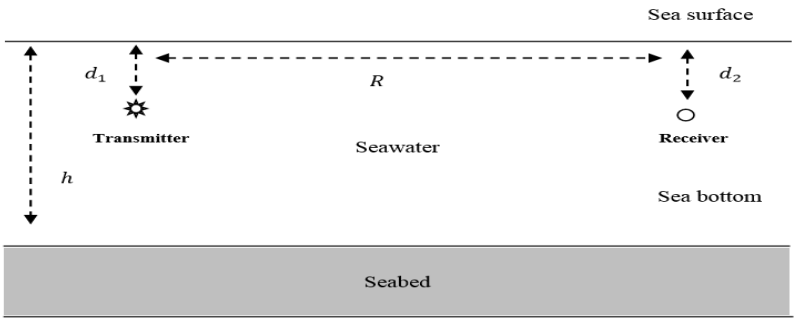

Figure 3. Schematic showing a Pekeris waveguide model of the shallow water acoustic channel

where d_1 is the depth of the source, d_2 is the depth of the receiver, h is the height of the water column and R is the transmission range. The distance travelled by the sound along various eigenrays can be computed using the method of images [7]. The distance along direct eigenray is denoted by D_{00} given by:

$$D_{00} = \sqrt{R^2 + (d_1 - d_2)^2} \tag{7}$$

where D_{sb} is the distance along an upward originating eigenray with s as surface reflections and b as bottom reflections. For such eigenrays, $0 \leq s - b \leq 1$ and:

$$D_{sb} = \sqrt{R^2 + [2bh + d_1 - (-1)^{s-b} d_2]^2} \tag{8}$$

where D_{bs} is the distance along a downward originating eigenray with s as surface reflections and b as bottom reflections. For such eigenrays, $0 \leq b - s \leq 1$ and:

$$D_{bs} = \sqrt{R^2 + [2bh - d_1 + (-1)^{b-s} d_2]^2} \tag{9}$$

3.1. Reflection at the Sea Surface

The impedance mismatch between the sea water and air causes the sea surface to be a very good reflector. If the sea surface is calm, the reflection is close to perfect but includes a phase shift by π radians i.e. the reflection coefficient is -1. If the sea surface is rough (due to waves), a small loss will be incurred for every surface interaction [13].

$$L_{SR} = -\exp\left(-0.5\,\Gamma^2\right) \tag{10}$$

where L_{SR} is the surface reflection coefficients and

$$\Gamma = 2k\sigma\sin\left(\theta\right) \tag{11}$$

$$\sigma = \sqrt{0.324.10^{-5}.v_w^5} \tag{12}$$

where k is acoustic wave length ($^{2\pi}/_{\lambda}$), θ is incident angle, σ is rms roughness of the surface and $v_m$is the wind speed in m/s.

3.2. Reflection at the Sea Bottom

The impedance mismatch between the sea water and seabed causes the sea bottom to reflect some of the sound incidents on it. Where ρ and c are the density and sound speed in sea water respectively and ρ_1 and c_1 are the density and sound speed in the seabed respectively. For a smooth sea bottom, the reflection is angle dependent and is given by the Rayleigh reflection coefficient [13, 14] as :

$$L_B(\theta) = \left|\frac{m\cos\theta - \sqrt{n^2 - sin^2\theta}}{m\cos\theta + \sqrt{n^2 - sin^2\theta}}\right| \tag{13}$$

where

$$m = \frac{\rho_1}{\rho}, n = \frac{c}{c_1} \tag{14}$$

The angle of incidence θ can be computed based on the geometry of the Pekeris waveguide. Let angle θ_{sb} correspond to an eigenray D_{sb} and angle θ_{bs} correspond to an eigenrayD_{bs}. Then, we have:

$$\begin{aligned}\theta_{sb} &= \tan^{-1}\left[\frac{R}{2bh + d_1 - (-1)^{s-b}d_2}\right]\\ \theta_{bs} &= \tan^{-1}\left[\frac{R}{2bh - d_1 + (-1)^{b-s}d_2}\right]\end{aligned} \tag{15}$$

3.3. Grazing Angles

The angle with which each ray grazes the boundaries is usually termed as a grazing angle. This is quite important because of its influence on both the bottom and surface reflection coefficients [9].

$$\emptyset = 90 - \theta \tag{16}$$

where θ is the incident angle.

3.4. Propagation Delay

The delay of each reflected ray with respect to the direct path is related to differences in the lengths of different paths. Let us call τ_{sb} the propagation delay along the ray length D_{sb} and τ_{bs} the propagation delay along the ray length D_{bs}.

$$\tau_{sb} = \frac{D_{sb} - D_{00}}{c}, \tau_{bs} = \frac{D_{bs} - D_{00}}{c} \tag{17}$$

The propagation delay of secondary rays with respect to the direct ray is a very important parameter in the underwater channel that affects system performance because the delayed replicas of the receiver introduce interference intersymbol hence the need to reduce the rate of transmission [4, 9].

3.5. Multipath Channel Model

Let $x(t)$ be the signal transmission through the channel and $y(t)$ be the corresponding received signal. Ignoring the absolute propagation delay on the direct ray between transmitter and receiver and combining the formulas, then $y(t)$ is expressed as a function of $x(t)$ in the following way [9]:

$$y(t) = \frac{L_A(D_{00})}{D_{00}}x(t) + \sum_{s=1}^{\infty}\sum_{b=s-1}^{s}\frac{L_A(D_{sb})(L_{SR})^s\left(L_{BR}(\theta_{sb})\right)^b}{D_{sb}}x(t-\tau_{sb}) + \sum_{b=1}^{\infty}\sum_{s=b-1}^{b}\frac{L_A(D_{bs})(L_{SR})^s\left(L_{BR}(\theta_{bs})\right)^b}{D_{bs}}x(t-\tau_{bs}) \quad (18)$$

The channel impulse response for a time-varying multipath underwater acoustic channel can be expressed as [2]:

$$h(\tau,t) = \sum_{p} A_P(t)\delta(\tau-\tau_p(t)) \quad (19)$$

where $A_p(t)$ and$\tau_p(t)$ denote time-varying path amplitude and time-varying path delay respectively. Hence, each path of an acoustic channel acts as a low-pass filter.

4. Channel Measurements

Although it is known that the shallow water channel is dominated by time-varying multipath, very few measurements of the variability of the multipath structure are done.

4.1. Sounding Signal

Since a unit impulse is an unrealizable signal, engineers choose a practical input signal to the system that will lead to an accurate estimation of the system impulse response. Several signals are frequently employed, those being LFM (linear frequency modulated) chirp [15], white noise [16], and DSSS BPSK (direct sequence spread spectrum binary phase shift keying) signal [15, 17]. All signals possess acceptable autocorrelation properties as to approximate Dirac delta function closely. Autocorrelation that approximates the Dirac delta function is the test of goodness for a sounding signal. LFM chirp signal is less likely to appear randomly in any environment than the other signals [18]. Therefore, the LFM chirp signal was used as the sounding signal in the experiments presented later in this paper.

4.2. Impulse Response

For any linear system with impulse response $h(t)$ and input $x(t)$, the output $y(t)$ can be found by using convolution between input and impulse response of system [19].

$$y(t) = x(t) * h(t) \quad (20)$$

The input-output relationship defined according to the correlation function and the power spectrum is [20]:

$$R_{YY}(\tau) = h(\tau) * h(-\tau) * R_{XX}(\tau) \underset{F.T.}{\longrightarrow} S_{YY}(f) = |H(f)|^2 S_{XX}(f) \quad (21)$$

$$R_{YX}(\tau) = h(\tau) * R_{XX}(\tau) \underset{F.T.}{\longrightarrow} S_{YX}(f) = H(f) S_{XX}(f) \quad (22)$$

All the above relationships apply to sample functions and discrete-time signals. When the input signal is LFM signal, the autocorrelation of this signal is unit impulse signal and the Fourier transform (F.T.) of unit impulse signal is equal to one. Therefore, the result of cross-correlation between output and input represent the impulse response of the channel (multipath delay profile).

5. Sea Trial

5.1. Experimental Setup

The channel measurements were conducted on the 18th of June, 2014 (10 a.m.–12 p.m.) in Tanjung Balau, Johor, Malaysia (latitude: 1° 33.169′N; longitude: 104° 26.027′E). The chosen location has an average depth of about 22 m. Transmissions were made from an omni-directional transducer BII-8030 underwater acoustic transmitter with an available frequency range of 20 Hz to 100 kHz and a maximum cable length of 10 m. The signal was received using a broadband hydrophone (7 Hz–22 kHz) model DolphinEAR 100 Series). The maximum cable length was 30 m Figure 4. The wind speed was about 7 knots. The temperature at the sea surface was 28 °C, while the salinity was 35 ppt. Similarly, the speed of sound was 1541.3 m/s, as obtained using the Medwin equation.

The transmitted signal used was a 30 ms linear frequency modulation (LFM) signal with a bandwidth of 20 kHz centered around 40 kHz. The different transmission locations corresponded to 10 m and 100 m ranges. The received signal was sampled at 44 kbit/s and stored for later analysis. Figure 5 shows the experiment site.

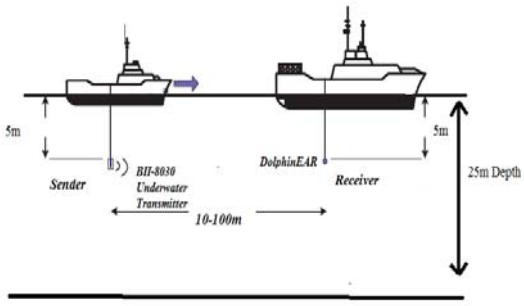

Figure 4. Configuration of the experiment at Tanjung Balau, Johor, Malaysia on June 18, 2014

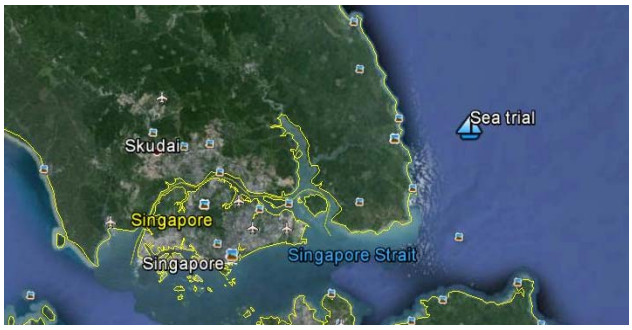

Figure 5. Experiment test site.

5.2. Results

The first test was conducted with a 10 m range at 22 m depth. The transducer and the hydrophone were submerged at 5 m depth. The LFM was sent, afterwhich, and the received signal was recorded at the receiver side. The cross-correlation process was performed between the transmitted and received signals using MATLAB to obtain the path delay profile. Figure 6 shows the multipath profile for 10 m range. The figure clearly showed that the grazing angle will increase when the distance between the sender and the receiver shortened, thereby decreasing the reflection coefficient. This result led the amplitude of the successive paths to quickly decrease and disappear.

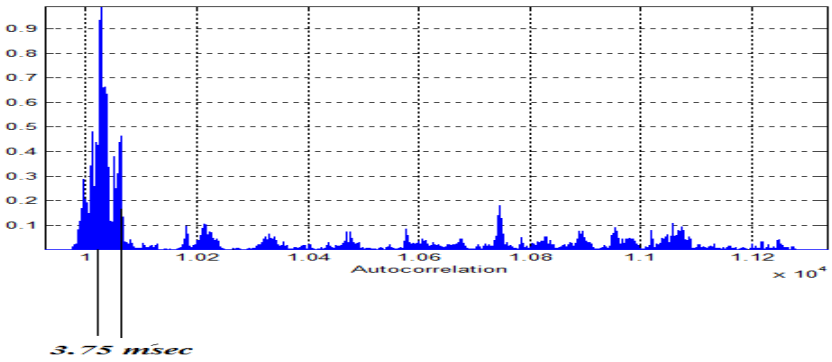

Figure 6. Multipath intensity profile at 10 m range

Figure 7 shows the results of the second test with 100 m range and 22 m depth. The transducer and the hydrophone were submerged at 10 m depth. The figure showed that the number of paths and the distance between the sender and the receiver increased when the range increased. Moreover, the grazing angle will decrease, thereby increasing the reflection coefficient. This result implied that the amplitude of the successive paths will not rapidly decline. The time difference between the different paths will be small. In other words, the successive paths will converge in time.

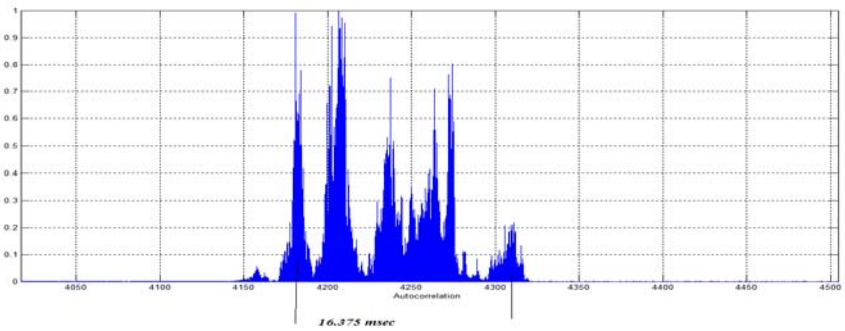

Figure 7. Multipath intensity profile at 100 m range.

Table 1 shows a comparison of the simulated delay depending on Eqs. (7), (8), (9), and (17) against the experimental propagation delay and the amplitude at each path arrival. The delay of each reflected ray was determined with respect to the direct path. The observation for the 100 m range was approximately the same as well as the propagation delay for rays hitting the surface or bottom, surface–bottom–surface, or bottom–surface–bottom, among others. This result was caused by the location of both the transmitter and the receiver being at nearly half of the channel depth.

Table 1. Comparison of the simulated against experimental propagation delay

Arrive number	Range (10 m)			Range (100 m)		
	Experiment delay($msec$)	Simulation delay($msec$)	Amplitude	Experiment delay($msec$)	Simulation Delay($msec$)	Amplitude
1	0	0	1	0	0	0.7
2	3.75	2.97	0.467	3.125	2.28	1
3	15.037	15.212	0.1	7	6.1	0.7517
4				10.375	12.2	0.7122
5				11.625	12.6	0.805
6				16.375	19.3	0.3018

6. Conclusion

The study considers the short-range shallow water hydroacoustic channel. The multipath effect in a shallow water channel has also been discussed. The numerical experiment results clearly show spatial variability in the acoustic signals, which are required for the design of shallow water communication systems. Multipath propagation keeps many hurdles in achieving high data rates and robust communication links. The delay spread of the channel significantly decreases in the case of short-distance links. Moreover, the effective data rate of this channel increases at a few hundred symbols per second.

Acknowledgements

The authors would like to thank the Universiti Teknologi Malaysia (UTM) and Ministry of Higher Education (MOHE) Malaysia for supporting this work.

References

[1] G Burrowes and JY Khan. *Short-range underwater acoustic communication networks*. INTECH Open Access Publisher. 2011.
[2] T Melodia, H Kulhandjian, LC Kuo and E Demirors. "Advances in underwater acoustic networking". *Mobile Ad Hoc Networking: Cutting Edge Directions*. 2013: 804-852.
[3] H Medwin and CS Clay. *Fundamentals of acoustical oceanography*. Academic Press. 1997.
[4] M Stojanovic and J Preisig. "Underwater acoustic communication channels: Propagation models and statistical characterization". *Communications Magazine, IEEE.* 2009; 47: 84-89.
[5] M Chitre, JR Potter and SH Ong. "Optimal and near-optimal signal detection in snapping shrimp dominated ambient noise". *IEEE Journal of Oceanic Engineering*. 2006; 31: 497-503.
[6] M Caley and A Duncan. "Investigation of underwater acoustic multi-path Doppler and delay spreading in a shallow marine environment". *Acoustics Australia.* 2013; 41: 20-28.
[7] Y Fei, L Xiao-Yang, W Qian and C En. "Underwater Acoustic Communication Based on Hyperbolic Frequency Modulated M-ary Binary Orthogonal Keying". *TELKOMNIKA Indonesian Journal of Electrical Engineering.* 2014; 12: 7311-7317.
[8] B Borowski. "*Characterization of a very shallow water acoustic communication channel*". in Proceedings of MTS/IEEE OCEANS. 2009.
[9] F De Rango, F Veltri and P Fazio. "A multipath fading channel model for underwater shallow acoustic communications". in *IEEE International Conference on Communications (ICC).* 2012: 3811-3815.
[10] WH Thorp. "Analytic Description of the Low-Frequency Attenuation Coefficient". *The Journal of the Acoustical Society of America.* 1967; 42: 270-270.
[11] FB Jensen. *Computational ocean acoustics*. Springer Science & Business Media. 1994.
[12] PC Etter. *Underwater acoustic modeling and simulation*. CRC Press. 2013.
[13] RP Hodges. *Underwater acoustics: Analysis, design and performance of sonar*. John Wiley & Sons. 2011.
[14] LM Brekhovskikh and IUrP Lysanov. *Fundamentals of ocean acoustics*. Springer Science & Business Media. 2003.
[15] S Dessalermos. "Undersea acoustic propagation channel estimation". Monterey, California. Naval Postgraduate School. 2005.
[16] P Schomer. "Measurement of Sound Transmission Loss by Combining Correlation and Fourier Techniques". *The Journal of the Acoustical Society of America*. 1972; 51: 1127-1141.
[17] M Chitre, J Potter and OS Heng. "Underwater acoustic channel characterisation for medium-range shallow water communications". in *OCEANS'04. MTTS/IEEE TECHNO-OCEAN'04*. 2004: 40-45.
[18] Y Fei, W Wen-Jun and C En. "Characteristics Analysis of HFM Signal over Underwater Acoustic Channels". *TELKOMNIKA Indonesian Journal of Electrical Engineering*. 2013; 11: 1173-1180.
[19] AV Oppenheim and GC Verghese. "Signals, systems, and inference". *Class notes for.* 2010; 6.
[20] PZ Peebles, J Read and P Read. *Probability, random variables, and random signal principles*. McGraw-Hill New York. 2001; 3.